Full Paper

Self-Assembled Multilayers of Polyethylenimine and DNA: Spectrophotometric and Electrochemical Characterization and Application for the Determination of Acridine Orange Interaction

*N. F. Ferreyra, G. A. Rivas**

INFIQC, Departamento de Fisicoquímica, Facultad de Ciencias Químicas, Universidad Nacional de Córdoba, Ciudad Universitaria, 5000-Córdoba, Argentina
*e-mail: grivas@fcq.unc.edu.ar

Received: January 5, 2009
Accepted: April 9, 2009

Abstract
This work deals with the study of the interaction between acridine orange (AO) and calf-thymus double stranded DNA (dsDNA) present in supramolecular architectures built on gold electrodes modified with mercapto-1-propanesulfonic acid (MPS) by self-assembling of polyethylenimine and dsDNA. The optimal conditions for building the supramolecular architecture were obtained from UV-vis spectrophotometric experiments. The electrochemical studies were performed by adsorptive transfer square wave voltammetry from the evaluation of the oxidation signal of AO accumulated within the multistructure. The effect of the number of PEI-dsDNA bilayers (Au/MPS/(PEI-dsDNA)$_n$) on the accumulation and electrooxidation of AO is also discussed.

Keywords: DNA, Polyethylenimine, Self-assembled multilayers, Acridine orange, Intercalation, Gold, DNA interaction

DOI: 10.1002/elan.200904593

1. Introduction

Since the discovery of the electroactivity of nucleic acids by Paleček [1], there has been an increasing interest in the development of electrochemical affinity biosensors based on the use of nucleic acids as recognition element. The combination of the biorecognition properties of nucleic acids with the known advantages offered by electrochemical techniques has resulted in highly successful biosensors [2–7]. These biosensors have been directed to gene analysis, detection of genetic disorders, tissue matching, DNA damage, and forensic applications [8].

Several approaches have been used for nucleic acids immobilization, the most relevant being: self-assembling of thiolated oligonucleotides on gold surfaces [9, 10], attachment of biotinylated oligonucleotides on avidin modified surfaces [11], covalent binding on chemically derivatized surfaces [11], adsorptive accumulation on electrode surfaces [12, 13], immobilization through polymeric matrices [14], and electrostatic self-assembling of multilayers [15, 16]. Among them, the self-assembling of multilayers by layer-by-layer deposition has been successfully used to immobilize DNA on different surfaces [17].

One of the applications of electrochemical DNA-based biosensors is the detection of the DNA interaction with different compounds. Intercalation is a mode of interaction that involves the insertion of molecules with planar aromatic ring systems between DNA base pairs and is responsible for a variety of biological consequences [7]. For instance, the know intercalators acridine dyes have demonstrated to present mutagenic, carcinogenic, antibacterial and antiviral properties [18]. In particular, the interaction of acridine orange (AO) with synthetic and biological polyelectrolytes has been widely investigated, mainly due to its ability to interact with genetic material. Their similarity to several antibiotics, such as daunomycin or actinomycin, make them interesting model systems for studying a variety of (bio)-physicochemical problems [19]. Furthermore, acridine derivatives are in the vanguard of antitumor drugs, and like ethidium derivatives, they initially bind to the minor groove of the DNA double helix through counter ion displacement, before intercalating between base pairs [20, 21]. Therefore, the development of new strategies that allow the critical study of the interaction between AO and dsDNA and the highly sensitive electrochemical detection of AO accumulated within the double helix confined to an electrode, represent an interesting alternative for further applications of AO as redox indicator in the design of electrochemical hybridization biosensors.

The intercalation between different compounds and DNA has been studied using diverse platforms. Cordes and Rechnitz [22] have used gold electrodes modified with 5'-thiol-$(GC)_{10}$ double stranded DNA oligomers to study the electrochemical activity of redox couples in the presence of AO. Girousi et al. [23] have investigated the interaction of ethidium bromide and AO with DNA in solution using a

hanging mercury drop electrode. Fojta et al. [24] have studied the interaction between DNA and different intercalators by adsorptive transfer stripping AC voltammetry. The interaction of ethidium bromide and AO with DNA (double stranded, thermally denatured and supercoiled) has been studied by alternating current voltammetry at the hanging mercury drop electrode [24]. The cathodic adsorptive electrochemical behavior of cytosine and guanine in the presence of AO at the static mercury drop electrode has been also investigated [25]. Liu et al. [26] have studied the interaction of AO with DNA films prepared by layer-by-layer self-assembly of DNA and poly(allylamine) on quartz surfaces. Lvov et al. [27] have evaluated the formation of multilayers films of different nucleic acids with several polycations like polyallylamine, polyethylenimine, polylysine and polyarginine. The interaction of layer-by-layer deposited multilayer films of polydiallyldimethylammonium chloride (PDDA) and calf thymus DNA built on conducting (4-aminobenzoic acid-modified glassy carbon electrode) and non-conducting (quartz) substrates with methyl green have been also reported [27, 28]. In this work we propose the detection of the interaction of AO with dsDNA immobilized on gold electrodes by self-assembling of multilayers using the polycation polyethylenimine (PEI). The studies were performed by adsorptive transfer square wave voltammetry and the analytical signal of the interaction was the oxidation current of AO incorporated within the multilayer. Spectrophotometric experiments using a quartz surface were performed to select the optimum experimental conditions for the multilayer formation. To the best of our knowledge, this is the first contribution to the electrochemical determination of AO accumulated on the dsDNA immobilized at gold electrodes by self-assembling of multilayers.

2. Experimental

2.1. Reagents

Polyethylenimine (PEI) 50% w/v (Catalog number P-3143), single stranded calf thymus DNA (ssDNA) (lyophilized powder, Catalog number D8899), double stranded calf thymus DNA (dsDNA) (activated and lyophilized, catalog number D4522) were from Sigma. DNA stock solutions were prepared in water, while the dilutions were performed either in acetate (ionic strengths $\mu = 0.2$, pH 5.00) or in phosphate ($\mu = 0.2$ or $\mu = 0.1$) pH 7.50 buffer solutions. DNA concentration was determined by UV experiments using $\xi = 6000\ M^{-1}\ cm^{-1}$ [29]. Mercapto-1-propanesulfonic acid (MPS) and 3,6-bis(dimethylamino)acridine hydrochloride (acridine orange, AO) were from Aldrich. Other chemicals were reagent grade and used without further purification. All solutions were prepared with ultra-pure water (18 MΩ cm) from a Millipore MilliQ system.

2.2. Apparatus

2.2.1. Electrochemical Experiments

Electrochemical experiments were performed with an EPSILON potentiostat (Bioanalytical Systems Inc., USA). The electrodes were inserted into the cell (BAS, Model MF-1084) through holes in its Teflon cover. A platinum wire and Ag/AgCl, 3 M NaCl (BAS, RE-5B) electrodes were used as counter and reference electrodes, respectively. Gold disks of 3 mm diameter (CHI 101) were employed as working electrodes.

Preparation of the working electrode: The electrodes were first polished with alumina 0.05 μm for 2 min, followed by a careful sonication in deionized water for 5 min, immersion in "Piranha" solution (1 : 3 H_2O_2(30% v/v)/ H_2SO_4 (98% w/v)) for 10 min, and final rinsing and sonication with ultra-pure water. *Caution: Piranha solution is very corrosive and must be handled with care.* The clean surfaces were stabilized by cycling the potential between 0.200 V and 1.650 V at 10 V s^{-1} in a 0.50 M sulfuric acid solution until obtaining a reproducible response. Before each experiment, a cyclic voltammogram at 0.100 Vs^{-1} was performed in 0.50 M sulfuric acid solution to check the surface conditions and to obtain the electroactive area. This area was measured by integration of oxides reduction charge, assuming 420 μC per square centimeter of real area [30].

Modification of the working electrode: The first step in the preparation of the working electrode was the adsorption of the thiol onto the clean gold surface by soaking the electrode for 30 min in a 2.0×10^{-3} M MPS solution (prepared in 1.6×10^{-3} M sulfuric acid solution), followed by a careful rinsing with deionized water. Thiol adsorption produces a negatively charged surface due to the exposure of sulfonate groups. The following steps consisted of immersion for 20 min in aqueous solutions of 2.0 mg/mL PEI (prepared in water) and the adsorption of dsDNA (or ssDNA) prepared in 0.10 M phosphate buffer solution pH 7.50 ($\mu = 0.2$) for 60 min. After each immersion step, the electrode was copiously rinsed with the same buffer used to prepare the dsDNA solution. The multilayered structures were obtained by alternate immersions in PEI and dsDNA. The resulting electrodes are indicated as Au/MPS/$(PEI\text{-}dsDNA)_n$, being n the number of PEI-DNA adsorbed bilayers.

Acridine orange interaction: Electrodes modified with the desired number of layers were immersed in a fresh AO solution under magnetic stirring for 30 min at open circuit potential and then copiously rinsed with a 0.10 M phosphate buffer solution pH 7.50 ($\mu = 0.2$). Blank experiments were performed by immersing the electrodes in the buffer solution using the same experimental conditions.

After the interaction with AO, the electrochemical transduction was performed by Square Wave Voltammetry (SWV) in a 0.10 M phosphate buffer solution pH 7.50 ($\mu = 0.2$) at room temperature between −0.200 V and 1.250 V, with a pulse amplitude of 25 mV, a frequency of 10 Hz, and a potential step of 4 mV.

2.2.2. UV-Vis Experiments

The experiments were performed with a Shimadzu UV 1601 Spectrophotometer and a quartz cuve of 0.1 cm of optic way. To prepare the multilayer assembly, the internal quartz surface (Q) was treated to expose negative charges by sonication for 20 min in NaOH 1.0 % w/v in ethanol aqueous solution 59% v/v. PEI was adsorbed by filling the cuve with a 2.0 mg/mL aqueous solution for 20 min. Adsorption of dsDNA was done in a similar way from a solution of the desired concentration for 120 min. After each immersion step, the cell was copiously rinsed with buffer solution and the spectral curves were collected between 190 and 800 nm in a fresh buffer solution. Alternated contact with PEI and dsDNA solutions allowed the generation of the multilayered structures with the desired number of bilayers, n (Q/PEI-dsDNA)$_n$). To analyze the dsDNA adsorption time, the procedure was similar although DNA was self-assembled for different times on Q modified with one layer of PEI.

To study the interaction of AO with dsDNA, the modified quartz surfaces with the desired number of self-assembled bilayers were filled with a fresh solution of AO for 30 min followed by careful rinsing with 0.10 M phosphate buffer solution pH 7.50 ($\mu = 0.2$). Spectral curves were recorded in 0.10 M phosphate buffer solution pH 7.50. The concentration of AO intercalated (C_{AO}) was calculated form the absorbance at 499 nm where dsDNA does not contribute to the absorption and considering an extinction coefficient of 55 000 M^{-1} cm^{-1} [31].

To study the interaction in solution, the desired quantity of AO was added to a 2.6×10^{-4} M (85 ppm) dsDNA solution prepared in 0.10 M phosphate buffer pH 7.50 ($\mu =$ 0.2) and the spectral curves were recorded.

In all cases the baseline was obtained by using the selected buffer solution (either 0.10 M phosphate pH 7.50 or 0.10 M acetate pH 5.00). All experiments were performed at room temperature.

3. Results and Discussion

The building of PEI-dsDNA multilayers was evaluated spectrophotometrically following the dsDNA absorption band at 258 nm (PEI does not absorb at this wavelength). The interaction of AO with the confined dsDNA was evaluated both, spectrophotometrically, from the absorbance of AO, and electrochemically from the oxidation signal of AO.

3.1. Spectrophotometric Results

3.1.1. Characterization of the PEI-dsADN Self-Assembled Multilayer

Figure 1A shows a plot of absorbance as a function of the adsorption time of dsDNA and PEI on a Q surface during the building of the supramolecular architecture Q/(PEI-dsDNA)$_n$. The absorbance at 258 nm increases with the number of dsDNA layers, although the time necessary to reach the steady-state (saturation) value and the changes between these stationary values depend on the number of the DNA layer that is adsorbed. For instance, when dsDNA is adsorbed on Q/PEI (first layer of dsDNA), the change in the absorbance is 0.0212, while when dsDNA is adsorbed on Q/(PEI-dsDNA)$_1$/PEI (second layer of dsDNA), it is 0.0828, that is, almost four times higher than the increment observed after the adsorption of the first layer of dsDNA.

On the other hand, the kinetics for the adsorption of dsDNA also depends on the structure where the dsDNA is adsorbed. For instance, for the first (Q/(PEI-dsDNA)) and second (Q/(PEI-dsDNA)$_2$) DNA layers, the absorbance reached the stationary values after 10 and 115 min of dsDNA adsorption, respectively; while for the third, fourth and fifth bilayers, the saturation (steady-state) values of absorbance are reached for times longer than 120 min. These results are a clear indication that the organization of the supramolecular structure becomes more complex when the number of bilayers increases, probably due to the formation of some intermixed layers.

Figure 1B compares the variation of the absorbance with the number of PEI-dsDNA layers for supramolecular architectures prepared in buffer solutions of pH 5.00 and 7.50. In both cases, there is an almost linear relationship between the absorbance and the number of bilayers, indicating that there is no desorption of dsDNA during the deposition of the next PEI layer onto it. The absorbances at pH 7.50 are more elevated, demonstrating that a higher amount of dsDNA is immobilized under these conditions due to the increase in the negative charge density of the sugar-phosphate backbone that facilitates the electrostatic interaction with PEI.

The effect of the ionic strength of the dsDNA solution (prepared in phosphate buffer solution pH 7.50) on the construction of the supramolecular architecture was also evaluated (not shown). At variance with the linear increment obtained when using $\mu = 0.2$, there is an exponential increase of the absorbance with the number of adsorbed bilayers when $\mu = 0.1$. These results confirm the importance of the ionic strength when developing multistructures, in agreement with previous reports for other polymers [32].

3.1.2. Interaction dsDNA-AO

Spectrophotometric measurements allow distinguishing if AO is present in a monomeric form or as aggregates. According to the literature [31], the absorption spectrum of dilute AO solutions presents a band at 492, called α band attributed to the absorbance of AO in its electrostatically charged monomeric form ($pK\alpha = 10.4$ [33]). As AO concentration increases, the spectrum is gradually substituted by a new one with a maximum at 465 nm (β band) ascribed to the dimmer formation through $\pi - \pi$ interaction or stacking complex. Figure 2A shows absorption spectra for two concentrations of AO in phosphate buffer solution. For 44 μM AO (dashed line), the spectrum presents two

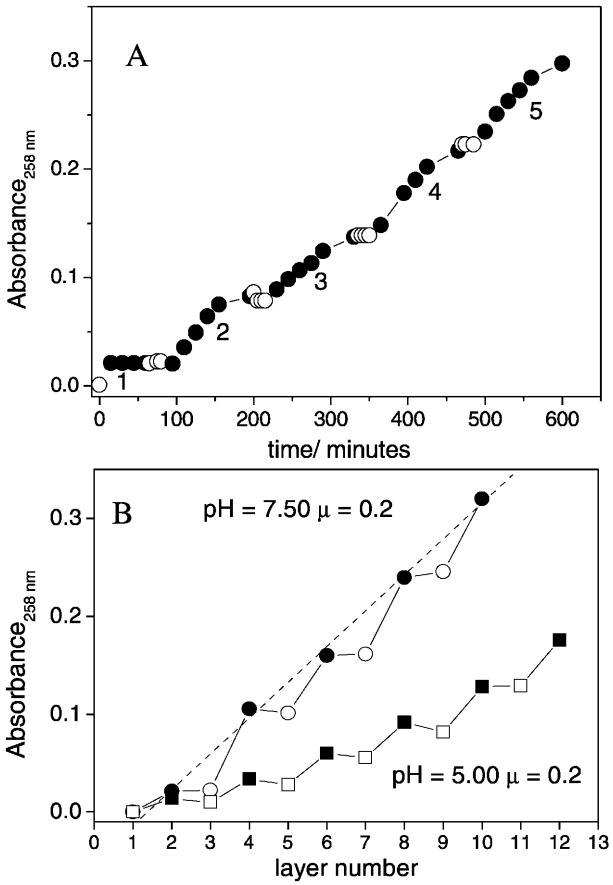

Fig. 1. A) Kinetic of dsDNA adsorption and B) variation of A_{max} vs. layer number using 3.3×10^{-4} M dsDNA (100 ppm) in phosphate buffer solution $\mu = 0.2$, pH 7.50 (circles) or acetate $\mu = 0.2$, pH 5.00 (squares). Closed and open symbols correspond to multilayer structures ended in dsDNA or PEI respectively.

absorption peaks at 230.5 nm and at 268 nm, and a broad one with two contributions at lower energies. From these two contributions, the most important is the one at 490.5 nm, denoting a high proportion of AO monomeric form. For 88 μM AO (solid line), the AO bands appears at 230 nm and 267 nm, while the maximum contribution in the broad peak at lower energies is the one at 470 nm, suggesting the dimmer formation.

When mixing AO and dsDNA solutions, the resulting absorption spectrum strongly depends on the dsDNA and AO concentrations ratio (C_{dsDNA}/C_{AO}). Figure 2B shows the spectral curves for a solution containing 2.6×10^{-4} M dsDNA in the absence (dotted line) and in the presence of increasing concentrations of AO. A typical profile was obtained for dsDNA alone with a maximum absorbance at 259.5 nm. For $C_{dsDNA}/C_{AO} = 30$ (solid line), the spectrum shows two bands, at 259.5 nm and at 501.5 nm. The first one involves contributions of both, dsDNA and AO, while the second one corresponds to the AO α band. The red shift of this band is an evidence of the intercalation of the monomeric form of AO within the dsDNA [29, 34]. For intermediate values, $C_{dsDNA}/C_{AO} = 3$ (dashed line), the interaction AO-dsADN occurs by intercalation in the double strand, with high affinity, and also through electrostatic interaction with dsDNA phosphate groups, with a low affinity constant [35]. Under these conditions, the presence of dimmers or higher associated forms is not significant, since the most important contribution in the broad peak is still the one at lower energies. At the lowest ratio, $C_{dsDNA}/C_{AO} = 0.6$ (dashed-dotted line), a signal at 467 nm is observed, which corresponds to the formation of AO dimmers [29]. Under these conditions, the intercalated monomeric form of AO, the AO electrostatically associated to dsDNA, and dimmers of AO are present, being this last contribution the most important.

Figure 2C shows absorption spectra obtained in phosphate buffer solution after the interaction of dsDNA confined to the Q surface (Q/(PEI-dsDNA)) with AO in solution. Under these conditions it is possible to evaluate the intercalation of AO within the double helix, since the AO electrostatically adsorbed to the phosphate groups of dsDNA is removed during the exhaustive rinsing with buffer solution. The spectral curves obtained in phosphate buffer solution after the interaction of 4.4 μM AO with Q/$(PEI\text{-}dsDNA)_2$ (2bl) present absorption peaks at 271.0 nm and 499.5 nm. These results demonstrate that, under these experimental conditions, AO effectively intercalates within the dsDNA confined to the multilayer. When the number of dsDNA layers raises the spectrum obtained for Q/$(PEI\text{-}dsDNA)_4$ (4bl) evidences the increase in the amount of AO accumulated within the multistructure. The surface concentration of dsDNA was obtained through the absorbance at 258 nm from similar experiments performed with 1.67×10^{-4} M dsDNA, in the absence of AO. For higher number of bilayers, the surface ratio C_{dsDNA}/C_{AO} decreases (36 for 4 bl, and 46 for 2 bl) due to the increase in the amount of AO present in the supramolecular architecture. In both cases, a red shifting is observed in the α absorption band, demonstrating that, under these experimental conditions, AO is effectively intercalated within the dsDNA confined to the multilayer. It is important to remark that unspecific adsorption of AO on Q/PEI was not detected (not shown).

3.2. Electrochemical Characterization

Spectrophotometric determinations has been useful to evaluate the formation of the multilayers system, to know the amount of DNA immobilized layer-by-layer and to demonstrate the presence of AO intercalated within the dsDNA confined to the supramolecular architecture. Electrochemical experiments provide additional information about the charge transfer of the intercalated AO.

Figure 3A and B show square wave voltammograms for different concentrations of AO at bare gold electrodes. The voltammogram obtained in phosphate buffer solution present a signal at around 0.95 V due to the gold oxides formation (dashed line, voltammogram I). In the presence of 1.0 μM AO, there is a broad peak at 0.8 V due to the oxidation of AO (II). For higher AO concentrations up to 100 μM, the current of this peak remains almost constant,

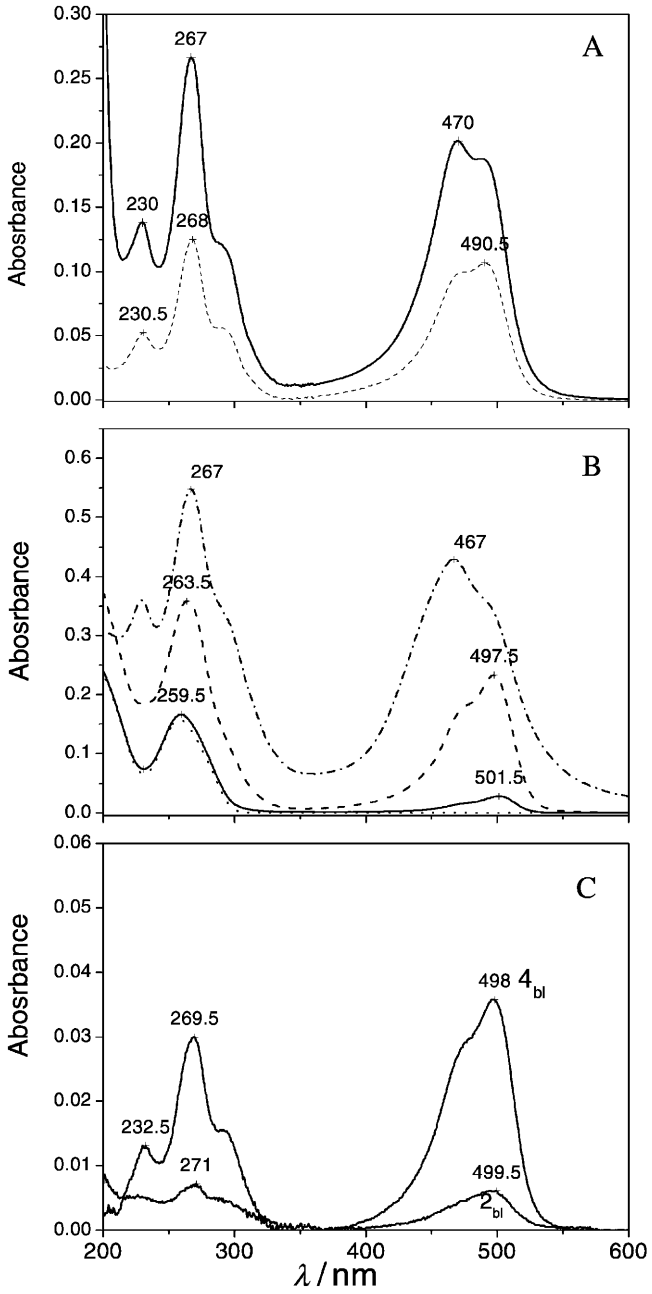

Fig. 2. Spectral curves obtained in phosphate ($\mu = 0.2$, pH 7.50) corresponding to: A) AO solution 8.8×10^{-5} M (—) and 4.4×10^{-5} M (---); B) 2.6×10^{-4} dsDNA solution plus AO: 0 M (·····), 8.8×10^{-6} M (—), 8.8×10^{-5} M (---), 4.4×10^{-4} M (-·-·-), and C) Q/(PEI-dsDNA)$_n$ with 2 (2bl) and 4 (4bl) bilayers post interaction with AO 4.4×10^{-5} M.

and a new small signal appears at 0.67 V. According to the spectrophotometric results shown before and previous reports [35], the peak at 0.8 V can be associated to the oxidation of the AO monomer, while the one at lower potentials, can be associated to the oxidation of the dimeric form. For AO concentrations higher than 100 μM the peak at 0.8 V becomes broader, including the small signal at lower potentials. The currents increase proportionally to the amount of AO with a small shifting in the peak potential (up to 0.84 V). At such AO concentrations higher associated forms of AO are also present.

Figure 4A shows square wave voltammograms obtained in phosphate buffer solution after the interaction of different electrodes at open circuit potential with 8.8×10^{-5} M AO for 30 min (selected from the spectrophotometric experiments). The results represent the average of the response obtained at four fresh electrodes. At Au/MPS (dotted line) and Au/MPS/PEI (dashed line), no response for AO was observed, indicating that AO can not be accumulated. The voltammograms obtained in phosphate buffer solution at Au/MPS/(PEI-dsDNA)$_n$ for $1 \leq n \leq 4$ (solid lines), show an oxidation signal at 0.84 V that increases almost linearly with the number of PEI-dsDNA bilayers up to the third one and more slowly after that (see inset). Similar trend was observed for experiments performed with AO 1.0×10^{-3} M (not shown). These results are a clear indication that AO can be strongly intercalated within the double helix of DNA at Au/MPS/(PEI-dsDNA)$_n$ multilayer, and that the accumulated AO can be electrooxidized. The electron transfer between the electrode and AO molecules intercalated within the double helix probably occurs through a hopping mechanism between the redox centers. As the number of bilayers increases, the AO oxidation signal does not increase in a linear way. This fact could be associated to a more difficult accessibility of AO to the dsDNA within the multilayer system and/or to a less efficient charge transfer of the AO accumulated in the external layers of the multistructure located far from the electrode surface. The spectrophotometric results showed that the amount of dsDNA as well as the quantity of AO accumulated within the multistructure increases with the number of layers. Therefore, the small increase in the electrochemical signal observed after the third bilayer, could be mainly associated to a less efficient electrooxidation of AO molecules.

Figure 4B shows the variation of AO peak current at 0.84 V as a function of the AO concentration for multistructures containing 2, 4 and 6 PEI-dsDNA bilayers after subtracting the corresponding buffer signal obtained from equivalent experiments where the interaction was performed by immersing the electrodes in buffer solution. As it was previously described, for n $\geq$ 3 the amount of AO accessible for oxidation does not increase linearly with the number of bilayers in the self-assembled structure. For this reason the results of figure 4B are normalized to the peak current obtained in phosphate buffer solution after the interaction with AO 5.0×10^{-5} M. Independently of the bilayer number, a fast saturation is observed for AO concentrations higher than 5.0×10^{-4} M.

The interaction of AO with a multilayer system prepared with ssDNA was also evaluated. Figure 5 displays the SWV responses obtained in phosphate buffer solution after the interaction of 8.8×10^{-5} M AO at open circuit potential at Au/MPS/(PEI-DNA)$_n$ prepared with ssDNA. At variance with the behavior observed at the architecture prepared with dsDNA, at Au/MPS/(PEI-ssDNA)$_n$, the peak current for AO remains the same for 1 and 2 bilayers, and decreases

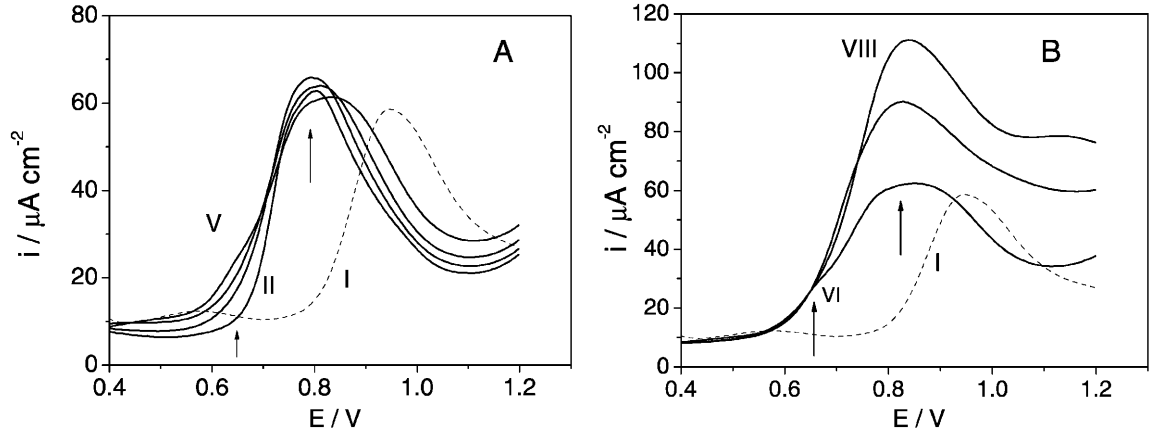

Fig. 3. A) and B) SWV at bare gold electrode of AO 0 μM (I), 1 μM (II), 25 μM (III), 50 μM (IV), 100 μM (V), 200 μM (VI), 1000 μM (VII), and 2000 μM (VIII). Supporting electrolyte: phosphate buffer solution ($\mu = 0.2$, pH 7.50).

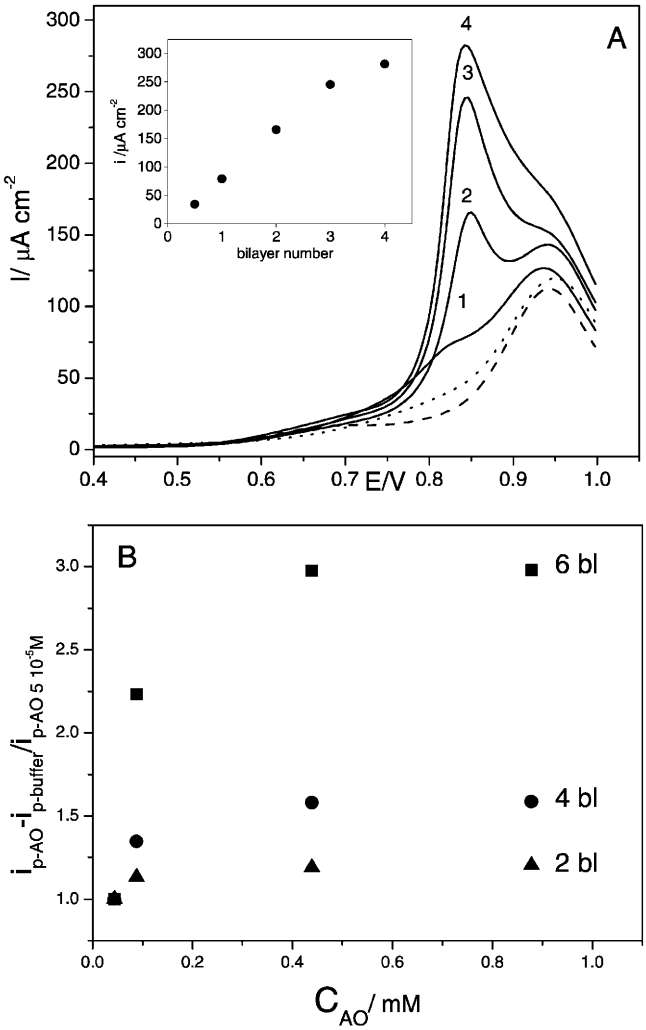

Fig. 4. SWV obtained in phosphate buffer solution ($\mu = 0.2$, pH 7.50) at Au/MPS (·····); Au/MPS/PEI (---) and Au/MPS/(PEI-dsDNA)$_n$ (—) after the interaction for 30 min at o.c.p. with 8.8×10^{-5} M AO (n is 1, 2, 3 or 4 bilayers). Inset: AO oxidation current at 0.84 V as a function of the adsorbed bilayer number. B) Normalized peak current as a function of AO concentration for Au/MPS/(PEI-dsDNA)$_n$ containing 2, 4 or 6 bilayers. Supporting electrolyte phosphate buffer solution ($\mu = 0.2$, pH 7.50).

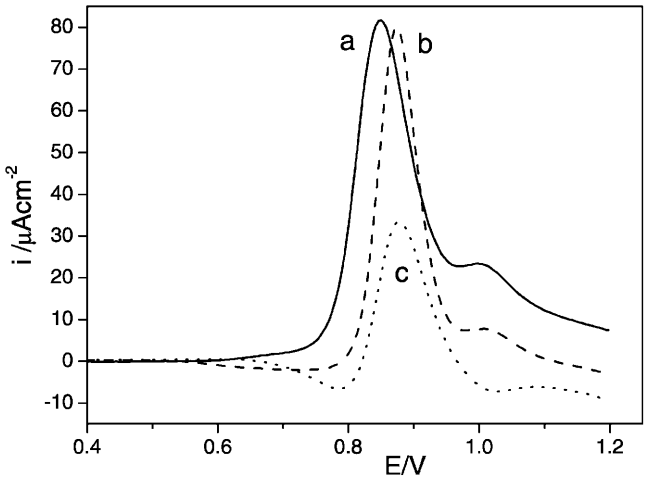

Fig. 5. SWV obtained in phosphate buffer solution ($\mu = 0.2$, pH 7.50) at Au/MPS/(PEI-DNA)$_n$ after the interaction with AO 8.8×10^{-5} M for 30 min at o.c.p. for bilayers prepared 100 ppm ssDNA100 where n is a) one (—), b) two (---) or c) four (·····) bilayers. In all cases the signal corresponding to the buffer was subtracted.

for 4 bilayers. Since the intercalation does not occur at ssDNA, the main mode of interaction is electrostatic, through the negative charges of the ribose-phosphate backbone. These results are in agreement with the model proposed by Decher et al. [36] to describe polyelectrolyte multilayers film. According to this model, is expected that negative charges of the ribose-phosphate backbone of the inner layers be neutralized; consequently, the electrostatic interaction with AO decreases, and for four bilayers the response is even smaller.

4. Conclusions

Self-assembled multilayers of PEI-dsDNA were efficiently adsorbed on quartz surfaces and MPS-modified gold electrodes. Spectrophotometric determinations provided

information about the kinetics for the formation of the multilayers system, the amount of DNA immobilized layer-by-layer and the presence of AO intercalated within the dsDNA confined to the supramolecular arquitecture. The pH and ionic strength of the dsDNA solution demonstrated to be an important variable for building the supramolecular multistructures.

Square wave voltammetry determinations, obtained from the oxidation signal of AO, demonstrated that the amount of AO accumulated within the Au/MPS/(PEI-dsDNA)$_n$ increases linearly with the number of PEI-dsDNA bilayers up to three, and that for higher number of bilayers the accessibility of the intercalated AO for electrooxidation is more difficult. The selectivity of the interaction between AO and dsDNA was demonstrated by comparing the response at a multilayer system prepared with ssDNA. These results represent an important contribution since, to the best of our knowledge, this is the first contribution that reports the electrochemical determination of AO accumulated on the dsDNA immobilized at gold electrodes by self-assembling of multilayers.

5. Acknowledgements

The authors thank CONICET, SECyT-UNC, Banco Santander Río, ANPCyT (Argentina) for the financial support.

6. References

[1] E. Paleček, *Nature* **1960**, *188*, 656.
[2] W. Zhao, J.-J. Xu, H.-Y. Chen, *Electroanalysis* **2006**, *18*, 1737.
[3] M. U. Ahmed, M. M. Hossain, E. Tamiya, *Electroanalysis* **2008**, *20*, 616.
[4] K. J. Odenthal, J. J. Gooding, *Analyst* **2007**, *132*, 603
[5] S. S. Babkina, G. K. Budnikov, *J. Anal. Chem.* **2006**, *61*, 728.
[6] G. A. Rivas, M. L. Pedano, N. F. Ferreyra, *Anal. Lett.* **2005**, *38*, 2653.
[7] G. A. Rivas, M. L. Pedano, *Encyclopedia of Sensors*, Vol. 3, *Electrochemical DNA Based Biosensors* (Ed: A. Craig, E. Grimes, C. Dickey, M. V. Pishko), American Scientific Publishers, New York **2006**, pp. 45 – 92.
[8] F. Lucarelli, S. Tombelli, M. Minunni, G. Marrazza, M. Mascini, *Anal. Chim. Acta* **2008**, *609*, 139.
[9] M. Trefulka, N. Ferreyra, V. Ostatná, M. Fojta, G. Rivas, E. Paleček, *Electroanalysis* **2007**, *19*, 1334.
[10] X. Wei, Q. Hao, Q. Zhou, J. Wu, L. Lu, X. Wang, X. Yang, *Electrochim. Acta* **2008**, *53*, 7338.
[11] A. Sassolas, B. D. Leca-Bouvier, L. J. Blue, *Chem. Rev.* **2008**, *108*,109.
[12] M. L. Pedano, G. A. Rivas, *Sensors* **2005**, *5*, 424.
[13] M. L. Pedano, L. I. Pietrasanta, M. L. Teijelo, *Electroanalysis.* **2008**, *20*, 739.
[14] S. Bollo, N. F. Ferreyra, G. A. Rivas, *Electroanalysis***2007**, *19*, 833.
[15] N. F. Ferreyra, S. Bollo, G. A. Rivas, unpublished results.
[16] M. L. Pedano, L. Martel, J. Desbrieres, E. Defrancq, P. Dumy, L. Coche-Guerente, P. Labbé, J. F. Legrand, R. Calemczuk, G. A. Rivas, *Anal. Lett*. **2004**, *37*, 2235.
[17] K. Ariga, J. P. Hill, Q. Ji., *PhysChemChemPhys.* **2007**, *9*, 231.
[18] P. Belmont, J. Bosson, T. Godet, M. Tiano, *Anti-Cancer Agents in Medicinal Chemistry*, **2007**, *7*, 139.
[19] N. J. Wheate, C. R. Brodie, J. G. Collins, S. Kempa, J. R. Aldrich-Wright, *Mini-Rev. Med. Chem.* **2007**, *7*, 627.
[20] J. M. Crenshaw, D. E. Graves, W. A. Denny, *Biochemistry* **1995**, *34*, 13682.
[21] P. A. M. Farias, A. de Luca Rebello Wagener, A. Aguiar Castro, M. B. R. Bastos, *Anal. Lett.* **2005**, *38*, 1601.
[22] R. E. P. Cordes and Garry A. Rechnitz, *Electroanalysis* **2000**, *12*, 351.
[23] I. Ch. Gherghi, S. T. Girousi, A. N. Voulgaropoulos, R. Tzimou-Tsitouridou, *Talanta* **2003**, *64*,103.
[24] M. Fojta, L. Havran, J. Fulnecková, T. Kubicarová, *Electroanalysis* **2000**, *12*, 926.
[25] P. A. M. Farias, A. de Luca, R. Wagener, A. A. Castro, *Anal. Lett.* **2005**, *38*, 1611.
[26] J. Lang, M. Liu, *J. Phys. Chem. B* **1999**, *103*, 11393.
[27] G. B. Sukhorukov, H. Möhwald, G. Decher, Y. M. Lvov, *Thin Solid Films* **1996**, *284 – 285*, 220.
[28] L. Luo, J. Liu, Z. Wang, X. Yang, S. Dong, E. Wang, *Biophys. Chem.* **2001**, *94*, 11.
[29] F. Zimmermann, B- Hossenfelder, J. C. Panitz, A. Wokaum, *J. Phys. Chem.* **1994**, *98*, 12796.
[30] R. Wood, *Chemisorption at Electrodes, Electroanalytical Chemistry* (Ed: A. J. Bard), Plenum Press, New York **1974**, ch. 9.
[31] L. Costantino, G. Guarino, O. Ortona, V. Vitagllano, *J. Chem. Eng. Data* **1984**, *29*, 62.
[32] G. Decher, in *Multilayers Thin Films. Sequential Assembly of Nanocomposite Materials*, (Eds: G. Decher, J. B. Schlenoff), Wiley-VCH, Weinheim **2003**, ch. 1.
[33] R. D. Falcone, N. M. Correa, M. A. Biasutti, J. J. Silber, *Langmuir* **2002**, *18*, 2039.
[34] J. C. Powers, Jr., W. L. Peticolas, *J. Phys. Chem* **1967**, *71*, 3191.
[35] M. B. Lyles, I. L. Cameron, *Biophys. Chem.* **2002**, 96, 53.
[36] G. Ladam, P. Schaad, J. C. Voegel, P. Schaaf, G. Decher, F. Cuisinier, *Langmuir* **2000**, *16*, 1249.

